SERI/PR-0-90154
(DE82016854)

AMORPHOUS BORON-SILICON-HYDROGEN ALLOYS FOR THIN-FILM HETEROJUNCTION SOLAR CELLS

Final Report for the Period June 1, 1980—May 31, 1981

By
A. R. Moore
D. E. Carlson
R. W. Smith

July 1981

Work Performed Under Contract No. AC02-77CH00178

RCA Laboratories
Princeton, New Jersey

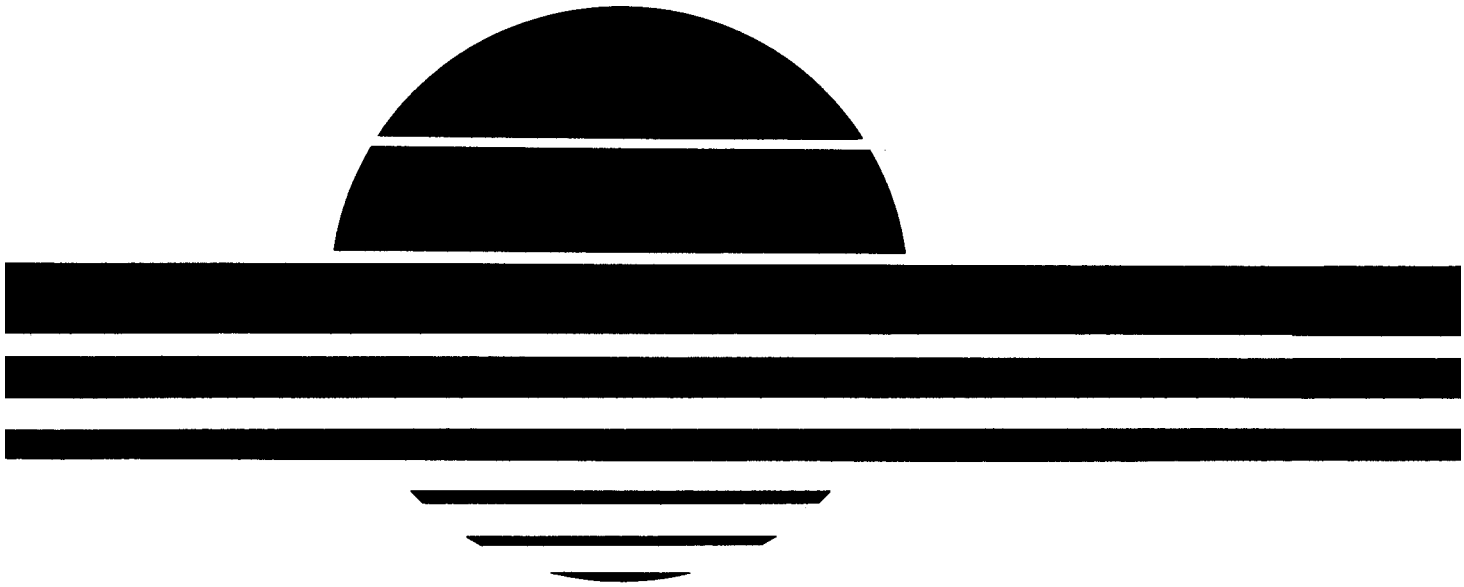

U.S. Department of Energy

Solar Energy

DISCLAIMER

SERI/PR-0-9010-4
(DE82016854)
Distribution Category UC-63

AMORPHOUS BORON-SILICON-HYDROGEN ALLOYS FOR THIN-FILM HETEROJUNCTION SOLAR CELLS

Final Report
for the period 1 June 1980 to 31 May 1981

July 1981

A. R. Moore
D. E. Carlson
R. W. Smith

RCA Laboratories
Princeton, New Jersey 08540

Prepared under Subcontract
No. XS-0-9010-6
for the

Solar Energy Research Institute
A Division of Midwest Research Institute
1536 Cole Boulevard
Golden, Colorado 80401

PREFACE

This Final Report covers the work performed by the Display and Energy Systems Research Laboratory of RCA Laboratories, Princeton, New Jersey for the period 1 June 1980 to 31 May 1981 under Contract No. XS-0-9010-6. The Laboratory Director is Brown F Williams; D. E. Carlson is the Group Head and A. R. Moore is the Project Scientist.

The contract objectives are to deposit amorphous boron-silicon-hydrogen (a-B:Si:H) and microcrystalline silicon-carbon-hydrogen (m-Si:C:H) alloys in a dc glow-discharge system, to characterize these films as a function of deposition conditions, to fabricate heterojunction devices using these materials and a-Si:H, and to characterize these devices.

SUMMARY

Amorphous boron-silicon-hydrogen (a-B:Si:H) films have been grown in dc proximity glow discharges in atmospheres containing B_2H_6, SiH_4, and H_2. The films are p-type and exhibit conductivities as high as $\sim 3 \times 10^{-4}$ $\Omega^{-1}cm^{-1}$. The conductivity of a-B:Si:H films increases with substrate temperature and annealing temperature for temperatures up to 500°C (highest investigated). However, increasing the conductivity causes the optical gap to decrease.

Amorphous boron-silicon-hydrogen alloys have been used to make heterojunction contacts to hydrogenated amorphous silicon (a-Si:H) films. The best conversion efficiency for these heterojunction devices is ~1.65% as compared to ~5.5% for a-Si:H p-i-n devices made in the same system with similar deposition conditions. The performance of a-B:Si:H/a-Si:H heterojunction cells appears to be limited mainly by a large density of interface states that act as trapping and recombination centers.

We also investigated another p-type, wide bandgap material, namely, microcrystalline silicon-carbon-hydrogen (m-Si:C:H). We explored three techniques to make m-Si:C:H films: glow-discharge deposition, thermal annealing of a-Si:C:H films, and laser annealing of a-Si:C:H films. While our results indicate that laser annealing is the most promising approach, the formation of microblisters prevented us from fabricating devices.

TABLE OF CONTENTS

LIST OF ILLUSTRATIONS

SECTION 1.0

INTRODUCTION

The major goal of this program was to develop a new wide-bandgap p-type material that could be used to fabricate an efficient heterojunction/amorphous silicon solar cell. While p-i-n a-Si:H solar cells have exhibited conversion efficiencies in excess of 6.0%, the quality of the doped layers, especially the p layer, is poor. The optical gap of p-type a-Si:H (~1-3 at.% boron) is ~1.4 eV [1] so that a significant fraction of the incident light is absorbed in even a thin top p layer. Moreover, the recombination lifetime appears to be very short so that most photogenerated carriers in the p layer recombine and do not contribute to the short-circuit current density, J_{sc}.

As described in our previous reports [2-4], we have been investigating p-type a-B:Si:H as a material for forming a good heterojunction to a-Si:H. However, recent data indicated that interface states are adversely affecting device performance [3,4]. We also explored the possibility of developing another p-type, wide bandgap material based on a silicon-carbon-hydrogen alloy in the microcrystalline state (m-Si:C:H).

Carbon alloying of a-Si:H films causes the optical gap to increase [5], but preliminary data indicate that these a-Si:C:H alloys are relatively resistive even when doped with boron or phosphorus. On the other hand, crystalline SiC is a wide bandgap semiconductor ($E_g \simeq 3.0$ eV) that can be doped either p or n type. Thus we attempted to make doped microcrystalline Si:C:H films with the hope of obtaining both a wide bandgap and good conductivity. We have tried to make m-Si:C:H films using glow discharge deposition, thermal annealing, and laser annealing.

SECTION 2.0

DEPOSITION CONDITIONS

Most of the a-B:Si:H films were grown in a dc proximity discharge mode with an applied voltage of 900 to 1000 V and a current density of 0.16 mA/cm^2 to the cathodic screen. The substrates were positioned ∿1.3 cm below the cathodic screen, and the anode screen was ∿1.3 cm above the cathode (see Fig. 2-1). The discharge atmosphere usually consisted of mixtures of SiH_4 and 15.4 vol% B_2H_6 in H_2. The pressure was ∿0.65 Torr and the flow rate, 70 standard cm^3 per minute (sccm). Some films were made in discharges containing mixtures of SiF_4 and 15.4 vol% B_2H_6 in H_2. Other films were made in discharges containing various amounts of He and Ar in addition to B_2H_6, SiH_4, and H_2.

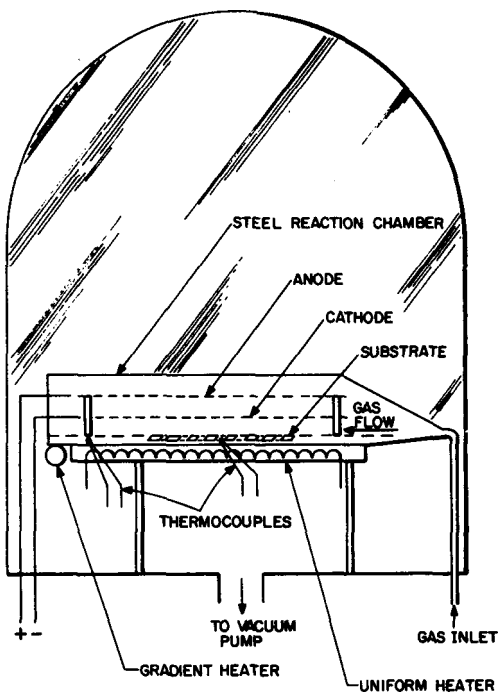

Figure 2-1. A diagram of the dc proximity glow-discharge deposition system.

The films were deposited on substrates in a temperature gradient running from 250 to 400°C over 9 cm. The gradient heater consisted of a stainless-steel

plate with a SiC glow bar located at one end of the plate. The glow bar was housed in a stainless-steel tube welded to the baseplate, and a fused silica tube was used to electrically isolate the glow bar. As shown in Fig. 2-1, the entire baseplate was contained in a stainless-steel reaction chamber with the gases admitted through a funnel at one end (the opposite end of the chamber was the exhaust port). A flow rate of 70 sccm was sufficient to prevent impurities from the heater or the outer bell jar walls from reaching the growing film. The reaction chamber was grounded, and the discharge electrodes were allowed to float; the anode was typically +80 V above ground.

Several substrates were used in each deposition run: a fused silica strip coated with Cr stripes (for conductivity measurements), two small fused silica plates (for optical absorption measurements), and two single-crystal silicon chips (for infrared absorption measurements). The fused silica strip was 10 cm long with Cr stripes ∿1.7 mm wide and ∿1.7 mm apart. The small fused silica plates and silicon chips were located near the hot and cold ends of the baseplate. The deposition rate varied from ∿50 nm/min at the cold end to ∿15 nm/min at the hot end. This variation appears to be caused by a gas depletion effect since the gas flows over the substrate from the cold to hot ends. For a geometry where the gas flows perpendicular to the substrate, the deposition rate was ∿47 nm/min at a substrate temperature (T_s) of 470°C and ∿6 nm/min at T_s = 240°C.

Recently, several investigators have shown that microcrystalline silicon-hydrogen (m-Si:H) films can be deposited from glow discharges at substrate temperatures below 400°C [6-8]. We have produced similar films using dc cathodic glow discharges in atmospheres containing SiH_4 diluted in H_2 and dopants such as PH_3 or B_2H_6. However, as discussed in Section 4.1, the addition of CH_4 or $Si(CH_3)_4$ suppresses the formation of microcrystallites, and the resulting-carbon-alloyed films are amorphous.

SECTION 3.0

AMORPHOUS BORON-SILICON-HYDROGEN ALLOYS

3.1 RESISTIVITY OF a-B:Si:H FILMS

The conductivity was measured in the dark by means of the four-probe technique. Figure 3-1 shows the conductivity obtained in typical gradient runs in which the boron concentration in the gas, $X_g = [B_2H_6]/([B_2H_6] + [SiH_4])$, ran from 0.5 to 0.95. The trend is that higher substrate temperatures and lower boron concentrations result in higher room-temperature conductivity. No measurements were made on samples of boron concentration lower than 50% because Tsai's results [9] showed that the situation reverses below this value, yielding lower conductivity. All samples were p type by thermoelectric power test.

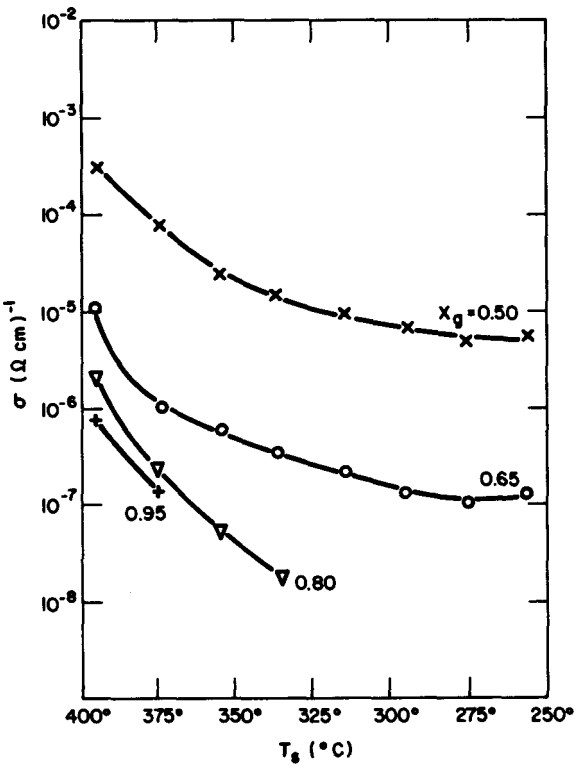

Figure 3-1. Conductivity as a function of substrate temperature for a series of a-B:Si:H films. $X_g = [B_2H_6]/([B_2H_6] + [SiH_4])$.

The conductivity was measured as a function of temperature for a number of representative samples. The logarithmic plots vs reciprocal temperature do not give straight lines over a very large temperature range, as was also found by Tsai [9]. The high-temperature end near 500 K appears to be most representative of the activation energy for conduction in the extended states. In this range an activation energy of 0.32 eV was found for $X_g = 0.5$ and substrate temperature at 380°C, and over 0.4 eV for $X_g = 0.8$.

Several films were annealed for 15 minutes in H_2 at successively higher temperatures. Annealing treatments at temperatures in the range of ∿350 to ∿500°C caused the conductivity of films deposited at low substrate temperatures ($\lesssim$350°C) to improve significantly, but the effects were much smaller for the more conducting films produced at higher substrate temperatures (∿400°C). Figure 3-2 shows that while the conductivity of a film deposited at 375°C did improve by almost an order of magnitude after a 15-minute anneal at 400°C, the activation energy was essentially unchanged.

We have deposited a-B:Si:H and a-B:Si:H:F films from various discharge atmospheres; e.g., 15.4% B_2H_6 in H_2 and SiH_4; 15.4% B_2H_6 in H_2, SiH_4, and He; 15.4% B_2H_6 in H_2, SiH_4, and Ar; and 15.4% B_2H_6 in H_2 and SiF_4. In all cases the resistivity decreased as T_s increased, but we never measured $\rho < 10^3$ Ω·cm even for $T_s \sim 500$°C (most films were made with $X_g = 0.8$).

Figure 3-3 shows conductivity data as a function of substrate temperature (T_s) for a series of films made under varying conditions. As before, the parameter $X_g = [B_2H_6]/([B_2H_6] + [SiH_4])$ is used to quantify the amount of B_2H_6 in the discharge atmosphere. As shown in the figure, all the films exhibited similar conductivity behavior; increasing T_s caused the conductivity to rise significantly in all cases. There was little difference between films made in ac (60 Hz) or dc(P) discharges. Similar data were also obtained when the discharge atmosphere contained either 70 vol% He or Ar with $X_g = 0.8$. However, somewhat more resistive films were obtained when SiF_4 was substituted for SiH_4.

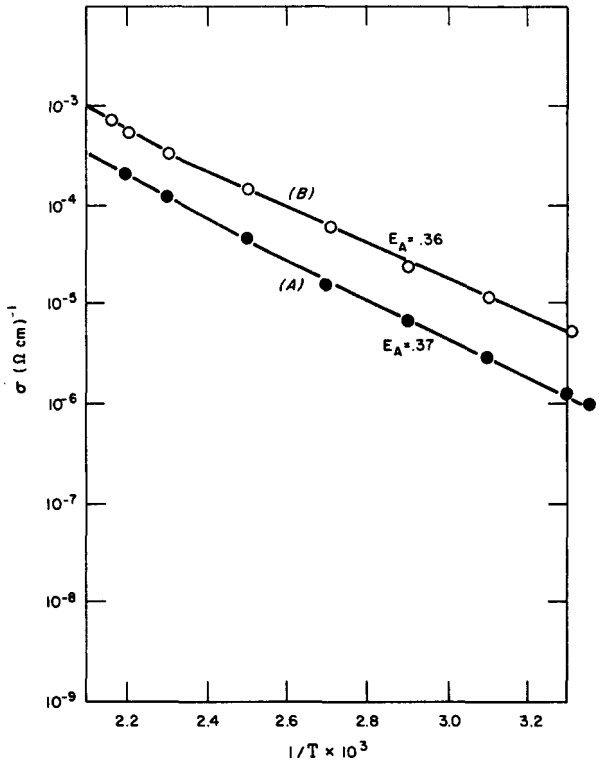

Figure 3-2. A semilog plot of conductivity as a function of $10^3/T$ for an a-B:Si:H film (A) before and (B) after a 15-minute anneal in H_2 at 400°C (X_g = 0.8).

More recently, we made a series of a-B:Si:H films by using discharge atmospheres containing 15.4% B_2H_6 in H_2, SiH_4, and H_2 so that the atmosphere contained ∿90 vol% H_2 (X_g = 0.8). Again the films were all relatively resistive with $\rho > 10^3 \Omega \cdot cm$ even at high T_s (∿500°C).

3.2 OPTICAL ABSORPTION

Figure 3-4 compares optical absorption data for an a-B:Si:H film (X_g = 0.8) and an a-Si:H film. Both films were made in a dc(P) discharge with substrate temperatures of ∿380 and ∿325°C, respectively. The data are similar to that obtained by Tsai [9]; the a-B:Si:H film exhibited reduced absorption in the

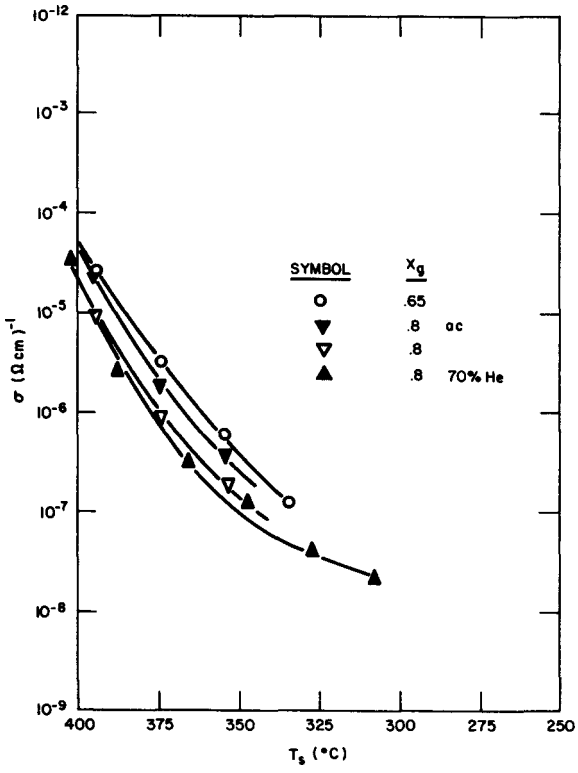

Figure 3-3. Conductivity as a function of substrate temperature for a series of a-B:SiH films made under varying deposition conditions.

visible light regime as compared to the a-Si:H film, but increased absorption in the near infrared ($h\nu < 1.9$ eV). The large absorption in the infrared is indicative of a large density of gap states, and this is confirmed by the absence of photoluminescence in the present a-B:Si:H films.

The data for the same a-B:Si:H film are replotted in Fig. 3-5 in the form of $(\alpha h\nu)^{1/2}$ vs $h\nu$ in order to estimate the optical gap. The value of $\varepsilon_{opt} \simeq 1.66$ eV is comparable to that of undoped a-Si:H films and is larger than that of p-type a-Si:H films containing a few at.% of boron ($\varepsilon_{opt} \simeq 1.4$ eV) [1]. The optical gap of a-B:Si:H films can be increased by increasing the boron content, but the conductivity decreases.

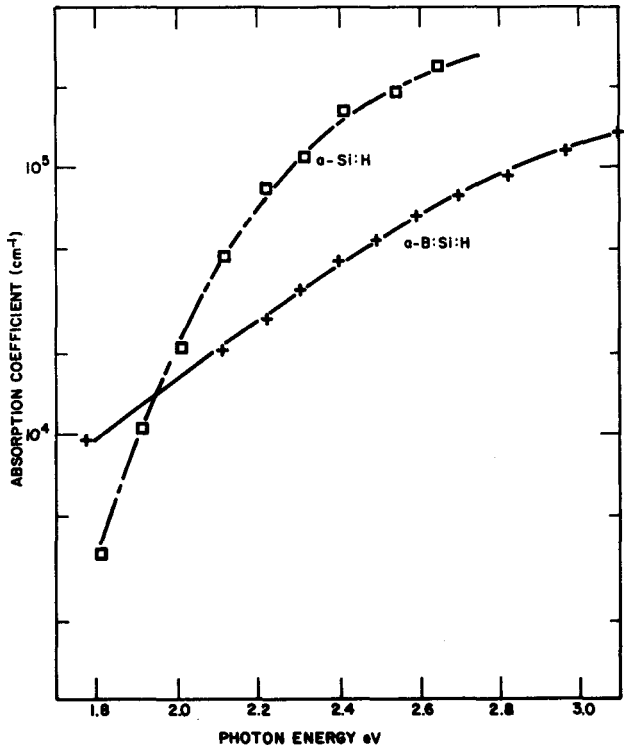

Figure 3-4. Absorption coefficient as a function of photon energy for an undoped a-Si:H film and an a-B-Si:H film (X_g = 0.8).

These a-B:Si:H films do not exhibit any significant photoconductivity or photoluminescence. (Persans et al. [10] also reported the absence of photoconductivity.) These results are not surprising in view of the large electron spin densities ($\sim 10^{18}$ to 10^{19} cm^{-3}) reported by Tsai [9].

3.3 COMPOSITIONAL DATA

Auger electron spectroscopy was used to obtain the compositional profile in Fig. 3-6. The film was deposited in a dc(P) discharge at $T_s \simeq 380°C$ with X_g = 0.8. The profile shows that the boron concentration is ~70 at.% and is relatively uniform throughout the film thickness. The hydrogen content was not determined for these films.

Figure 3-7 shows a similar profile for a film made in a discharge containing SiF_4 instead of SiH_4. In this case, the boron concentration does appear to

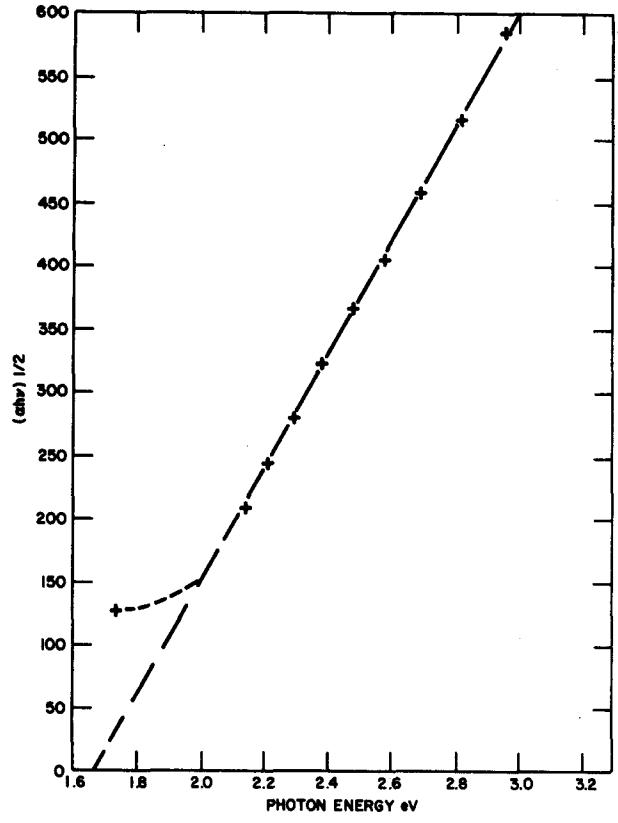

Figure 3-5. A plot of $(\alpha h\nu)^{1/2}$ as a function of photon energy for a-B:Si:H film (X_g = 0.8).

vary with thickness presumably due to varying discharge conditions, and the film contains ∿1 at.% fluorine (X_g = 0.5).

3.4 HETEROJUNCTION DEVICES

Several a-B:Si:H/a-Si:H heterojunction devices were made on stainless-steel substrates with electron-beam-deposited ITO as top contacts. Table 3-1 lists the photovoltaic characteristics of several heterojunction devices as well as those of control cells made entirely from a-Si:H. The first three devices listed had the structure ITO/n-i/p/steel where the p layer was either p-type a-Si:H ($B_2H_6/SiH_4 \simeq 1.3\times10^{-2}$) or a-B:Si:H ($X_g$ = 0.8). The second group of these devices was similar except the structure was inverted: ITO/p/i-n/steel.

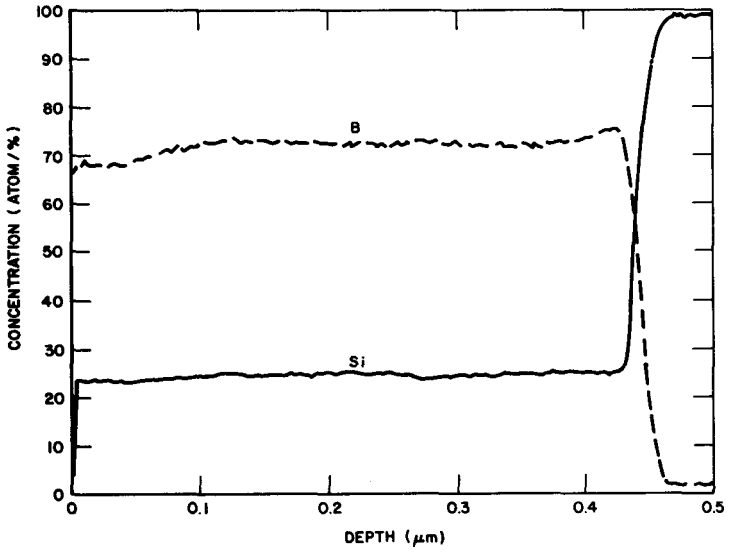

Figure 3-6. A compositional profile of an a-B:Si:H film (X_g = 0.8).

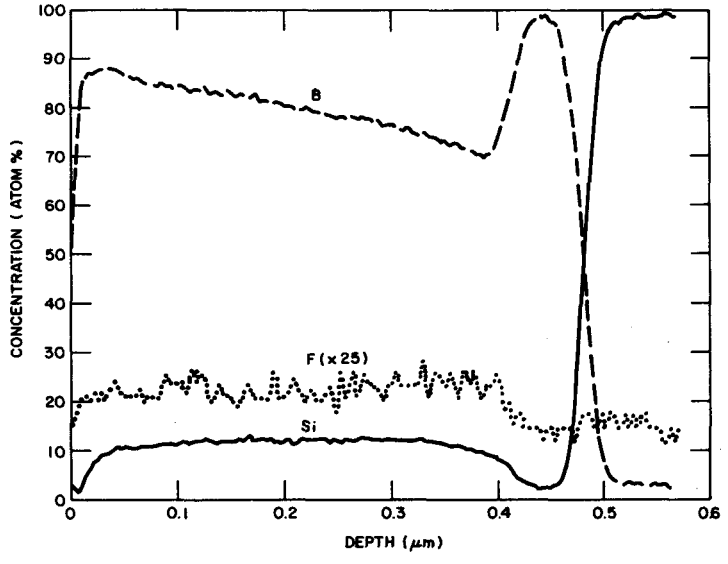

Figure 3-7. A compositional profile of an a-B:Si:F:H film (X_g = 0.5).

Table 3-1. PHOTOVOLTAIC PROPERTIES OF a-B:Si:H (X_g = 0.8) HETEROJUNCTION CELLS

Structure	V_{oc} (mV)	J_{sc} (mA/cm^2)	FF	η (%)
ITO/n-i-p/ss	809	12.35	0.546	5.46
ITO/n-i/a-B:Si:H/ss	628	4.69	0.334	0.98
ITO/n-i/←a-B:Si:H/ss	521	1.44	0.327	0.25
ITO/p-i-n/ss	590	10.01	0.548	3.24
ITO/a-B:Si:H/i-n/ss	751	3.29	0.328	0.81
ITO/a-B:Si:H/←i-n/ss	623	6.24	0.360	1.40

The data in Table 3-1 show that the device performance decreases dramatically when the p-type a-Si:H is replaced by p-type a-B:Si:H. In the first series of devices where the p layer is deposited first, all the photovoltaic parameters decrease, especially J_{sc}. In the second series where the n layer is deposited first, we actually see an improvement in V_{oc} for the heterojunction devices, but again J_{sc} and the fill factor show a significant decrease. Grading the undoped a-Si:H film into the a-B:Si:H layer improves the performance somewhat compared to an abrupt junction.

An array of a-B:Si:H/a-Si:H heterojunction devices was made by depositing the films on a stainless-steel substrate in a temperature gradient (running from ~250 to ~400°C), and then depositing small electrodes (5 mm^2) of indium-tin-oxide as the top contacts. We made one array with the structure ITO/a-B:Si:H/i-n a-Si:H/steel and another with the structure ITO/n-i a-Si:H/a-B:Si:H/steel. For the a-B:Si:H films we used a discharge atmosphere containing 15.4% B_2H_6 in H_2 and SiH_4 with X_g = 0.8. The n a-Si:H layer was made from a discharge containing 2% PH_3 in SiH_4. The discharge mode was dc proximity with 0.6-Torr pressure, 50-sccm flow, and a current density of 0.11 mA/cm^2 at the cathodic screen.

Figure 3-8 shows how the conversion efficiency of these two arrays varied with substrate temperature. In both cases, the efficiency falls off significantly as T_s increases above ~300°C. The best efficiency is ~1.65% for the case where the a-B:Si:H layer was deposited last and where T_s ~ 250-280°C. However, both J_{sc} and the fill factor are much lower than observed in similar structures with a p-type a-Si:H top layer (see Table 3-1).

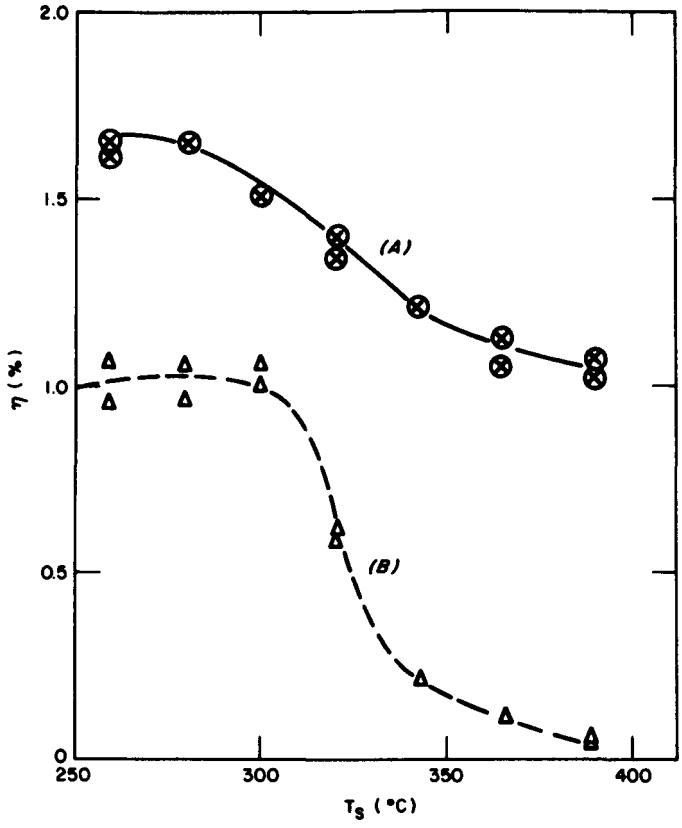

Figure 3-8. Conversion efficiency as a function of substrate temperature for two types of a-B:Si:H/a-Si:H heterojunction devices.

3.5 DISCUSSION

The performance of a-B:Si:H/a-Si:H heterojunction devices appears to be limited by a large density of interface states. These interface states apparently act

as traps and recombination centers and are probably related to the gap states in a-B:Si:H. Several experimental results indicate that the density of these gap states is relatively large. Tsai found that the ESR spin density of a-B:Si:H films was on the order of 10^{19} cm^{-3} [9] while values of $\sim 10^{15}$ to 10^{16} cm^{-3} have been reported for a-Si:H films [10]. Moreover, optical absorption data indicate a large absorption tail in the near infrared [3,9]. Finally, no photoluminescence has been observed in any of our a-B:Si:H films as mentioned in Section 3.2.

Another important factor is that our a-B:Si:H films have an optical gap comparable to that of undoped a-Si:H, and activation measurements for the conductivity indicate that the Fermi level is $\sim$0.35 to 0.40 eV above the valence band. Therefore, we cannot expect a large built-in potential from an a-B:Si:H/a-Si:H heterojunction.

Thus, we conclude that a-B:Si:H is not a suitable heterojunction material for fabricating efficient solar cells.

SECTION 4.0

MICROCRYSTALLINE SILICON-CARBON-HYDROGEN ALLOYS

4.1 GLOW-DISCHARGE DEPOSITION AND THERMAL ANNEALING

As discussed in Section 2.0 we have produced microcrystalline Si:H (m-Si:H) films using dc glow discharges where the substrate is the cathode and the discharge atmosphere contains ~10% SiH_4 in H_2; the doping levels were typically either $PH_3/SiH_4 \simeq 2\times10^{-2}$ or $B_2H_6/SiH_4 \simeq 1.3\times10^{-2}$.

Figure 4-1 (curve A) shows resistivity data for a film grown in a temperature gradient in a discharge containing 9 vol% SiH_4 in H_2 with a doping level of $B_2H_6/SiH_4 \simeq 1.3\times10^{-2}$. The total gas pressure was 2.5 Torr, and the flow rate was 150 sccm. The current density at the cathodic substrate was 1.1 mA/cm^2. As shown in the figure, the resistivity falls rapidly as the substrate temperature increases above ~350°C. Electron diffraction has shown that the high-resistivity material is amorphous while the low-resistivity material is microcrystalline.

We have found that the transition temperature (T_c) between the amorphous and microcrystalline regions depends strongly on the composition of the discharge atmosphere, but only weakly on the discharge power, pressure, and flow rate. The addition of tetramethylsilane, $Si(CH_3)_4$, to the discharge atmosphere inhibits the formation of microcrystalline material, and as shown in Fig. 4-1 (curve B), the resistivity remains high ($>10^2$ $\Omega\cdot cm$) even for T_s = 500°C when a small amount of $Si(CH_3)_4$ is added [$Si(CH_3)_4/SiH_4$ = 0.05].

We subsequently annealed this film for 15-minute intervals in forming gas (10% H_2, 90% N_2) at successively higher temperatures, and the resistivity data are shown in Fig. 4-1 as the high temperature extension of curve B. A large decrease in resistivity does not occur until the annealing temperature exceeds 800°C. Under similar conditions, a-Si:H films will crystallize at an annealing temperature of ~700°C. Hydrogen evolves from these films at temperatures above

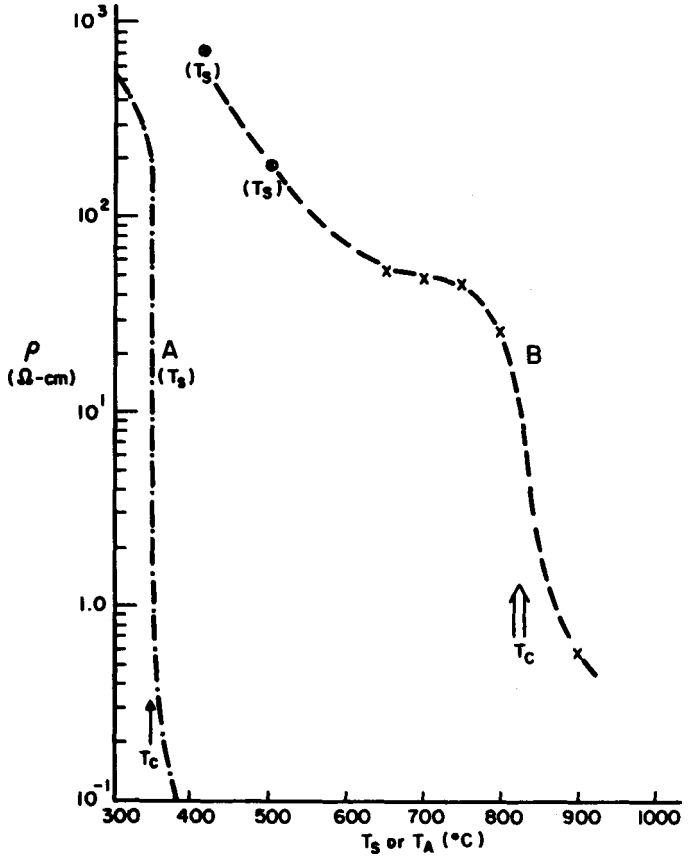

Figure 4-1. Resistivity as a function of either substrate temperature (T_S) or annealing temperature (T_A).

~350°C, and the hydrogen content is generally reduced by more than two orders of magnitude before crystallization occurs [12].

In another series of experiments, varying amounts of CH_4 were added to a discharge containing ~3.5 vol% SiH_2 in H_2 with $B_2H_6/SiH_4 \simeq 1.3 \times 10^{12}$. The films were all grown at 450°C in a dc cathodic discharge. As shown in Fig. 4-2, the resistivity of the films increases rapidly as the CH_4 content is increased. It is evident that the presence of CH_4 is suppressing the formation of microcrystalline films. A similar effect was observed with the addition of $Si(CH_3)_4$.

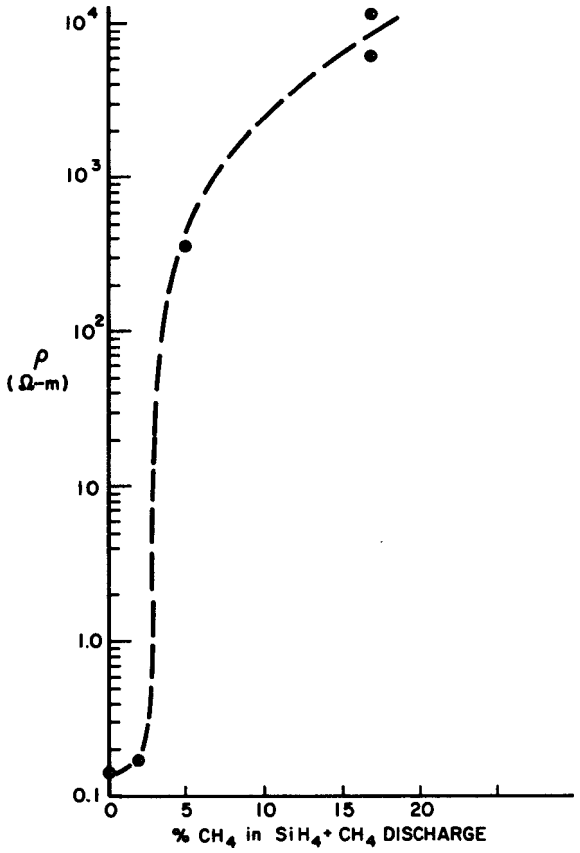

Figure 4-2. Resistivity as a function of the methane content of the discharge atmosphere.

4.2 LASER ANNEALING OF a-Si:C:H FILMS

Previous work has shown that laser annealing can be used to crystallize amorphous silicon films.* Thus, we exposed several a-Si:C:H films deposited on SiO_2 glass substrates to pulsed laser light (λ = 0.53 μm) from a Nd:YAG laser. The pulse width was 15 ns with a 10-Hz repetition rate while a raster was scanned. Resistivity data is listed in Table 4-1 for films before and after laser annealing at a power density of 0.1 J/cm^2. The large changes in resistivity (10^4 -10^5 X)

* J. I. Pankove, private communication.

are indicative of a transition from the amorphous to the microcrystalline state. In some regions the laser exposure caused discoloration of the films due to the formation of microblisters.

Table 4-1. RESISTIVITY OF Si:C:H FILMS BEFORE AND AFTER LASER ANNEALING

DISCHARGE ATMOSPHERE	T_s (°C)	ρ_{BEFORE} (Ω·cm)	ρ_{AFTER} (Ω·cm)
90% SiH_4 (1.3% B_2H_6), 10% $Si(CH_3)_4$	510	3.0×10^{2}	4×10^{-2}
90% SiH_4 (1.3% B_2H_6), 10% $Si(CH_3)_4$	370	4.8×10^{3}	4.3×10^{-2}
90% SiH_4 (2% PH_3), 10% $Si(CH_3)_4$	520	4×10^{3}	2.1×10^{-2}

Increasing the laser power to 0.15 J/cm^2 decreased the resistivity by an additional factor of ∿3-5. However, the visible damage to the films also increased.

In another series of experiments, we varied the laser power density from 0.09 to 0.15 J/cm^2 for sections of an a-Si:C:H film deposited on a stainless-steel substrate. In this case, the resistivity appeared to increase for all power densities and the film was visibly damaged in each case. Since the laser beam has a gaussian profile, the damage (microblisters) is most severe in the central region of the beam impact area. The increase in resistivity may be caused by microcracks in the film.

4.3 DISCUSSION

The results presented in Section 4.1 clearly indicate that the formation of microcrystalline material is inhibited by the presence of either CH_4 or $Si(CH_3)_4$

in the SiH_4 discharge. Moreover, the annealing experiments show that the presence of carbon in the a-Si:H matrix suppresses crystallization. Similar effects have been observed in amorphous silicon-carbon alloys made by chemical vapor deposition [13].

The major difficulty in using higher deposition temperatures (T_s > 500°C) to form m-Si:C:H films is that this precludes the use of many low-cost substrates such as steel or SnO_2-coated glass. The situation is even worse for microcrystalline films generated by thermal annealing (T_A ~ 900°C). Even if suitable substrates were used (e.g., possibly Mo), one might have to hydrogenate the films by exposing them to a hydrogen plasma (with T_s ~ 300-400°C) in order to obtain good electrical properties.

Laser annealing of a-Si:C:H films appears to offer the best method for obtaining m-Si:C:H films. The laser annealing process is extremely fast (~15 ns) and energy-efficient. However, the results of this study indicate that it is difficult to produce m-Si:C:H films by laser annealing without creating microblisters. For this reason we did not attempt to fabricate m-Si:C:H/a-Si:H heterojunction devices.

SECTION 5.0

REFERENCES

1. Carlson, D. E., Smith, R. W., Magee, C. W., and Zanzucchi, P. J. To be published in Philos. Mag.
2. Moore, A. R., Carlson, D. E., and Smith, R. W. Quarterly No. 1, SERI/PR-0-9010-1, prepared for the Solar Energy Research Institute under Subcontract No. XS-0-9010-6, September 1980.
3. Moore, A. R., Carlson, D. E., and Smith, R. W. Quarterly No. 2, SERI/PR-0-9010-2, prepared for the Solar Energy Research Institute under Subcontract No. XS-0-9010-6, May 1981.
4. Moore, A. R., Carlson, D. E., and Smith, R. W. Quarterly No. 3, SERI-PR-0-9010-3, prepared for the Solar Energy Research Institute under Subcontract No. XS-0-9010-6, June 1981.
5. Anderson, D. A. and Spear, W. E. Philos. Mag. 35, 1 (1977).
6. Usui, S. and Kikuchi, M. J. Non-Cryst. Solids 34, 1 (1979).
7. Matsuda, A., Yamasaki, S., Nakagawa, K., Okushi, H., Tanaka, K., Iizima, S., Matsumura, M., and Yamamoto, H. Jap. J. Appl. Phys. 19, L305 (1980).
8. Nagata, Y., Kunioka, A., and Yamazaki, S. Appl. Phys. Lett. 38, 142 (1981).
9. Tsai, C. C. Phys. Rev. B19, 2034 (1979).
10. Persans, P. D., Tsai, C. C., and Fritzsche, H. Bull. Am. Phys. Soc. 23, 310 (1978).
11. Fritzsche, H., Tsai, C. C., and Persans, P. D. Solid State Technol. 21, 55 (1978).
12. Magee, C. W. and Carlson, D. E. Solar Cells 2, 365 (1980).
13. Booth, D. C., Allred, D. D., and Seraphin, B. O. Solar Energy Materials 2, 107 (1979).

☆U.S. GOVERNMENT PRINTING OFFICE: 1982-546-085 77 REGION NO. 4